Biophysical Chemistry 41 (1991) 217–236
Elsevier Science Publishers B.V., Amsterdam

BIOCHE 01588

Effect of ethidium on the torsion constants of linear and supercoiled DNAs

Peng Guang Wu, Bryant S. Fujimoto, Lu Song and J. Michael Schurr

Department of Chemistry, BG-10 University of Washington, Seattle, WA 98195 (USA)

(Received 8 September 1989; accepted in revised form 11 March 1991)

Abstract

The torsion elastic constants (α) of linear pBR322 (4363 bp) and pUC8 (2717 bp) DNAs and supercoiled pBR322 and pJMSII (4375 bp) DNAs are measured in 0.1 *M* NaCl as a function of added ethidium/base-pair (EB/BP) ratio by studying the fluorescence polarization anisotropy (FPA) of the intercalated ethidium. The time-resolved FPA is measured by using a picosecond dye laser for excitation and time-correlated single photon counting detection. Previously developed theory for the emission anisotropy is generalized to incorporate rotations of the transition dipole due to excitation transfer. The excitation transfers are simulated by a Monte Carlo procedure (Genest et al., Biophys. Chem. 1 (1974) 266–278) and the consequent rotations of the transition dipole are superposed on the Brownian rotations. After accounting for excitation transfer, the torsion constants of the *linear* DNAs are found to be essentially independent of intercalated ethidium up to a binding ratio $r = 0.10$ dye/bp. Dynamic light scattering measurements on linear pUC8 DNA confirm that the torsion constant is independent of binding ratio up to $r = 0.20$ dye/bp. If α_d denotes the torsion constant between ethidium and a base-pair, and α_0 that between two base-pairs, then our data imply that α_d/α_0 lies in the range 0.65 to 1.64 with a most probable value of 1.0. The torsion constants of *supercoiled* DNAs decrease substantially with increasing binding ratio even after accounting for excitation transfer. At the binding ratio $r^* = 0.064$, where the superhelix density vanishes and superhelical strain is completely relaxed, the torsion constant of the supercoiled pBR322 DNA/dye complex lies below that of the corresponding linear DNA/dye complex by about 30%. This contradicts the conventional view according to which linear, nicked circular, and supercoiled DNA/dye complexes with $r = r^*$ should coexist with the same concentration of free dye, display the same distribution of bound dye, and exhibit identical secondary structures, twisting and bending rigidities, and FPA dynamics. These and other observations imply the existence of metastable secondary structure in freshly relaxed supercoiled DNAs. A tentative explanation is presented for these and other unexpected observations on supercoiled DNAs.

Keywords: Supercoiled DNAs; Linear DNAs; Torsion constants; Ethidium dye

1. Introduction

Intercalated ethidium dye is the most widely used and intensively studied molecular probe for DNA. Its popularity is due mainly to its rather large binding constant, its strongly enhanced visible fluorescence, and its action to reduce net twist (i.e. unwind), and simultaneously increase the writhe, of covalently closed circular DNAs. In the interpretation of many experiments on linear and supercoiled DNA/ethidium complexes, it is explicitly or implicitly assumed that the intercalated ethidium has no significant effect on the DNA secondary structure, apart from local un-

winding and extension of the helix, or on the bending and twisting rigidities of the DNA in its vicinity. Until now this critical assumption has not been rigorously tested for either linear or supercoiled DNAs, and is by no means universally accepted. Indeed, on the basis of X-ray crystal structures of ethidium complexed with dinucleoside phosphates, Sobell et al. [1] proposed that ethidium would intercalate at the site of a so-called β-kink, and further suggested that such a β-kink would exhibit a 10-fold lower than normal torsional rigidity. To address this and other important questions, we examine the torsion constant determined from time-resolved fluorescence polarization anisotropy (FPA) [2–6] and the apparent plateau diffusion coefficient (D_{plat}) at large scattering vector (**K**) determined from dynamic light scattering (DLS) [7–9] as a function of ethidium binding ratio (r = bound dye/base-pair) up to rather high levels. To extract a reliable torsion constant under such conditions, it is first necessary to develop a credible procedure for deconvoluting the effects of depolarization by excitation transfer between closely spaced intercalated ethidiums, as discussed below. This is the principal technical advance that enables the present test of the effects of ethidium on the torsional rigidities of linear and supercoiled DNAs.

1.1 Excitation transfer between intercalated ethidium dyes

Fluorescence depolarization by excitation transfer between intercalated ethidium dyes was originally studied in attempt to determine their unwinding angle [10–14]. In that work, the total anisotropy was assumed to be a simple product of factors for the contributions of Brownian motion ($r_B(t)$) and excitation transfer ($r_E(t)$), namely $r(t) = (2/5)r_B(t)r_E(t)$. Though plausible at the time, this assumption is seen to be incorrect in light of subsequent theoretical developments. In any case, the unwinding angles obtained from those fluorescence studies differ significantly from the presently accepted value, which was established by other techniques [15–17]. This discrepancy prompted a reexamination of the validity of Förster type transfer [18] between identical fluorophores [19], and of the magnitude of the local refractive index along the helix-axis [12]. Evidence was adduced that Förster theory greatly overestimates the incoherent transfer rate over very short distances (≤ 10 Å) between ethidiums in either DNA or glycerol, although some observations are compatible with the theory [19]. At present there is insufficient experimental evidence to decide at what, if any, distance Förster theory is valid for excitation transfer between intercalated ethidium molecules.

In order to assess the contribution of torsional deformations to the FPA and DNA/ethidium complexes at relatively high binding levels, it is necessary to take account of the effects of excitation transfer. Monte Carlo methods for simulating the excitation transfer process and its contribution to fluorescence depolarization were developed [10] and refined [12,14] by previous workers in this area. Their techniques are employed here to simulate excitation transfer, although the incorporation of such results into the theoretical anisotropy function follows a new prescription. Up to a binding ratio $r = 0.10$, we find that the time-resolved FPA of linear DNA can be quantitatively described by a proper superposition of the Brownian dynamics of the filament and Förster-type excitation transfer between intercalated ethidiums. Dynamic light scattering is employed as an independent probe for any change in the torsional rigidity of linear DNA induced by ethidium.

1.2 Linear DNAs

In recent work, it is shown that the torsional rigidity and dynamics of linear pBR322 DNA in 0.1 *M* NaCl are unaffected by intercalated chloroquine up to rather high binding ratios, $r = 0.19$ [5]. However, at low ionic strength (3 mM Tris), moderate chloroquine binding ratios induce a substantial (35–40%) decrease in the torsional rigidity of linear pBR322 DNA [20]. The evidently strong salt dependence of the effect induced in linear DNA by chloroquine, which intercalates as the doubly charged species, provides an additional reason to study the effect of ethidium, which is single charged. Here we find that the

torsion constant of linear pBR322 DNA in 0.1 *M* NaCl is unaffected by intercalated ethidium up to at least $r = 0.10$, and almost certainly up to $r = 0.20$.

1.3 Supercoiled DNAs

In recent work it is found that the torsional rigidities of supercoiled pBR322 DNAs with two different initial superhelix densities ($\sigma = -0.048$ and -0.083) in 0.1 *M* NaCl actually decrease somewhat with increasing intercalated chloroquine. [5] In each case, near the particular binding ratio $r = r^*$, where the superhelical strain is completely relaxed by intercalated dye, the torsional rigidity is significantly smaller (by $\sim 15\%$) than that of the corresponding linear DNA with the same binding ratio [5]. At low ionic strength (3 m*M* Tris), moderate chloroquine binding ratios have no effect on the torsional rigidity of supercoiled pBR322 DNA (initial superhelix density $\sigma = -0.048$), in contrast to the substantial reduction in torsional rigidity of the linear form [20]. Under these latter conditions the difference in torsional rigidity between the completely relaxed supercoiled DNA with $r = r^*$ and the corresponding linear DNA with the same binding ratio amounts to ~ 35–40% [20]. These pBR322 DNAs are sufficiently long that end-effects on the measured torsional rigidity are entirely negligible [6]. Hence, any differences in torsional rigidity between the completely relaxed supercoiled and linear forms of this DNA with the same binding ratio must be attributed to some other cause. As indicated in the subsequent discussion, such differences cannot exist when the tertiary structures are uncondensed and the secondary structures of the completely relaxed supercoiled and linear forms are both at equilibrium.

In view of the unexpected results obtained with chloroquine a detailed comparison of the effects of ethidium on the torsion constants of linear and supercoiled DNAs is warranted. Indeed, we find that the torsion constants of two different supercoiled DNAs decrease markedly with increasing bound ethidium. At $r = r^*$, the torsion constant of relaxed supercoiled pBR322 DNA is substantially lower than that of its corresponding linear DNA.

1.3.1 Topology, free energy, and binding isotherm of a supercoiled DNA

In order to better understand the present results and to appreciate in detail their implications, some pertinent background is necessary.

Each supercoiled DNA topoisomer exhibits a particular integral number of turns of one strand around the other, called the linking number l. In general, l is partitioned among twist T and writhe W (of the helix-axis), which obey the topological constraint [21,22]

$$l = T + W \tag{1}$$

The superhelix density of a topoisomer is defined by $\sigma = \Delta l / l_0$, where $\Delta l = l - l_0$ is its (normally negative) linking number difference, and l_0 is the non-integral equilibrium (or intrinsic) twist of the unstrained (nicked) circular molecule with N base-pairs. Unwinding ligands, such as ethidium, act to reduce l_0 and increase the superhelix density.

For sufficiently small superhelix densities, where the superhelical deformation is slight, the torsion and bending elastic constants of the filament must be identical to those of the corresponding linear DNA, and the deformational free energy must vary quadratically with the linking difference. A theoretical treatment of this circumstance is based on the results of analytical theory [23] and simulations [24–26] for the distribution of writhe in nicked circular DNAs, and yields an expression for the difference in deformational free-energy between topoisomers of sufficient length [5],

$$\Delta A = (E_T/\mathrm{N})(\Delta l^2 - \Delta m^2). \tag{2}$$

The twist energy parameter E_T is related to the microscopic torsion constant between base-pairs (α) and the effective force constant for writhe (κ_W) in open circular DNAs with the same N according to $E_\mathrm{T} = [(2\pi)^2/2k_\mathrm{B}T)(\alpha\kappa_W/(\alpha + \kappa_\mathrm{W})]$. κ_W is proportional to the bending constant between base-pairs (κ_β) and for DNAs of sufficient length ($N \gtrsim 6000$ bp) is related to the bending constant by [6,23] $\kappa_W = \kappa_\beta/[(0.095)(2\pi^2)]$. Equation (2) accounts well for the distribution of nearly relaxed topoisomers obtained by pro-

longed action of Topoisomerase I on plasmids of sufficient length [27–30]. If one further assumes that intercalated ethidium does not alter the twisting or bending rigidity of the DNA and does not condense its tertiary structure, then the adsorption isotherm of a supercoiled DNA near the relaxed limit, subject to nearest-neighbor exclusion, is [5]

$$r/C = K\ e^{a(r^*-r)}(1-2r)^2/(1-r) \qquad (3)$$

where r is the binding ratio (bound dye/base-pair), C is the concentration of free ethidium, K is the intrinsic binding constant, $r^* = \Delta l(360)/\phi N$ is the binding ratio at which the superhelix density vanishes ($\sigma = 0$) and the superhelical strain energy is completely relaxed (i.e. $\Delta A = 0$), and $a = 2E_T\,(\phi/360)^2$, where $\phi = 26°$ is the unwinding angle for ethidium [16,17]. At the binding ratio $r = r^*$, where the superhelix density is completely relaxed, eq. (3) becomes precisely the binding isotherm for linear or nicked circular DNA (i.e. $E_T = 0$). Indeed, at the relaxed condition, $r = r^*$, the linear, nicked circular, and relaxed supercoiled DNA/dye complexes are all predicted to equilibrate with the same concentration of free dye, to have the same distribution of bound dye, and to exhibit the same torsion and bending elastic constants, regardless of any effect of dye to alter those constants. Near the relaxed limit, these predictions must hold, provided that the tertiary structures remain uncondensed and that the secondary structures of the different species are all at equilibrium. The observation of different torsion constants for corresponding linear and supercoiled DNA/dye complexes with $r = r^*$ would imply that one or both of these species exhibits either some condensed tertiary structure and/or some metastable secondary structure.

We also inquire whether the assumptions upon which eqs. (2) and (3) are based remain valid up to larger negative superhelix densities in the intermediate ($\sigma \simeq -0.025$) and native ($\sigma = -0.05$) ranges. Indirect evidence that the domain of validity of eq. (2) does not extend to superhelix densities in the intermediate and native ranges has been reported [31,32]. Moreover, although experimental binding isotherms display the form predicted by eq. (3) and generalizations thereof over a wide range of negative and positive superhelix density [5,33–35], the E_T values inferred from such data are typically (i.e. more often than not) only about half or less of those ($E_T \simeq 1000$) obtained by analysis of relaxed topoisomer distributions using eq. (2) [5]. These reported failures of eqs. (2) and (3) could in principle be ascribed to (i) decreases in the torsion and bending elastic constants with increasing negative superhelix density (due to anharmonicity of the potential); (ii) changes in the equilibrium secondary structure with increasingly negative superhelix density; or (iii) a weaker than quadratic dependence of supercoiling free energy on the linking difference at constant equilibrium secondary structure and constant twisting and bending rigidity, or some combination of all three. Direct observation of a similar or larger torsion constant for the native supercoiled DNA compared to its corresponding linear form would rule out possibility (i). Direct observation of different responses of the torsion constants of supercoiled and linear DNAs to bound ethidium would suggest that possibility (ii) is in part responsible for the observed failures of eqs. (2) and (3) at intermediate and native superhelix densities.

2. Materials and methods

Supercoiled pBR322 (4363 bp) and pUC8 (2717 bp) DNAs were prepared as described earlier [36]. Supercoiled pJMSII (4375 bp) is a plasmid constructed from pBR322 by the insertion of two consensus binding sites for catabolite activator protein (CAP) [37,38], and is similarly prepared. Measurements of the superhelix densities, as described previously [5], yields $\sigma \simeq -0.048 \pm 0.005$ for pBR322 and a similar value for pJMSII. More than 90% of both samples are present in the supercoiled form. These DNAs were linearized using EcoRI restriction enzyme. The sample buffers are 0.1 M NaCl, 10 mM Tris, 1 mM EDTA, pH 8.5 for linear and supercoiled pBR322 DNA; 0.1 M NaCl, 10 mM Tris, 10 mM EDTA, pH 8.0 for linear pUC8 DNA; and 0.1 M NaCl, 10 mM Tris, 1 mM EDTA, pH 8.0 for super-

coiled pJMSII DNA. DNA concentrations are all in the range 0.04–0.05 mg/ml.

Time-resolved FPA measurements are performed using a synch-pump picosecond dye-laser system as the excitation source and time-correlated single-photon counting apparatus for detection. Details of the instrumentation and experimental protocol are described elsewhere [2,3,6]. Excitation is set at 575 nm and fluorescence emission is detected at 645 nm. Samples are thermostated at 20 °C.

Dynamic light scattering (DLS) experiments were performed using instrumentation and procedures described elsewhere [7,8]. Correlation functions were measured over the range of K^2 ($K \equiv$ scattering vector) from 0.5 to 20×10^{10} cm^{-2} using a He–Ne laser operating at 632.8 nm and an Ar-ion laser operating at 351.1 nm. However, it was not possible to perform DLS experiments on supercoiled DNAs using 351.1 nm radiation in the presence of either ethidium or chloroquine without inducing extensive nicking of the sample. This photochemical nicking was attenuated 30–50% by exhaustive O_2 removal (e.g. by purging with Ar, or by repeated freeze-pump-thaw cycles). The presence of scavengers for singlet oxygen (Na-benzoate) and photochemically produced radicals (L-ascorbic acid) had comparatively little effect in either the presence or absence of O_2. DLS experiments at 351.1 nm are reported here only for linear pUC8 DNA, not for any of the supercoiled DNAs. The sample studied by DLS was purged with Ar to remove O_2 and contained 15 m*M* Na benzoate. All DLS measurements were studied at 21 °C.

All samples are characterized before and after the optical experiments by electrophoresis in 1% agarose gels containing Tris-borate buffer (90 m*M* Tris, 90 m*M* boric acid, 2 m*M* EDTA) in the presence and absence of chloroquine. No changes resulting from the experiments reported here could be detected.

3. Theory

DNA is regarded as a deformable filament with mean local cylindrical symmetry. It is assumed to comprise a linear, but not necessarily always straight, array of identical rigid subunits, or disks, each of which is connected to its neighbors by identical Hookean twisting and bending springs. Each intercalated ethidium is assumed to be attached with unique orientation to a particular subunit, called a dye-subunit, to which a coordinate frame is rigidly attached. At time $t = 0$, an excitation appears on the initially excited dye-subunit. Depolarization of the subsequent emission at time t is due to reorientation of the transition dipole associated with the excitation. This occurs by Brownian rotation of the dye-subunit and simultaneously via excitation transfer to nearby dye-subunits with different orientations of the dye. We define the instantaneous excitation frame as follows. Its origin is taken to coincide permanently with that of the initially excited dye-subunit while its orientation at time t is that of the dye-subunit bearing the excitation at time t. As the excitation jumps to successive dye subunits, each of which is undergoing rotational Brownian motion, the instantaneous excitation frame merely undergoes corresponding rotations about its body-fixed symmetry and transverse axes. When these rotations of the excitation frame are (nearly) continuous Gaussian random processes, the theoretical optical anisotropy of intercalated ethidium is given by [39]

$$r(t) = \frac{I_{\parallel}(t) - I_{\perp}(t)}{I_{\parallel}(t) + 2I_{\perp}(t)} = r_0 \sum_{n=0}^{2} I_n C_n(t) F_n(t), \tag{4}$$

where $I_{\parallel}(t)$ and $I_{\perp}(t)$ are the fluorescence intensities with polarizations parallel and perpendicular, respectively, to that of an infinitely short exciting pulse. Unresolved rapid isotropic wobble of the dye is manifested simply as a reduction in r_0 [40]. The I_n are trigonometric functions

$$\begin{aligned} I_0 &= \left(\tfrac{3}{2}\cos^2\epsilon_0 - \tfrac{1}{2}\right)^2 \\ I_1 &= 3\cos^2\epsilon_0 \sin^2\epsilon_0, \\ I_2 &= \tfrac{3}{2}\sin^4\epsilon_0 \end{aligned} \tag{5}$$

where $\epsilon_0 = 70.5$ is the equilibrium polar angle

between the transition dipole and the helix-axis [40,41]. $C_n(t)$ is the twisting correlation function

$$C_n(t) = \left\langle \exp\left[-n^2 \frac{\langle \Delta_z(t)^2 \rangle}{2} \right] \right\rangle_R , \qquad (6)$$

and $F_n(t)$ is the tumbling correlation function

$$F_n(t) = \left\langle \exp\left[-(6-n^2) \frac{\langle \Delta x(t)^2 \rangle}{2} \right] \right\rangle_R , \qquad (7)$$

where $\langle \Delta_j(t)^2 \rangle$, $j = z$ or x, is the mean-squared angular displacement at time t of the excitation frame around its symmetry ($j = z$) or transverse ($j = x$ or y) axes. R denotes an average over all disks to which the dye could bind, and is irrelevant for long linear ($N + 1 \geq 2000$ bp) or circular DNAs, such as are considered here.

When the binding ratio is less than 1 ethidium per 150 bp ($r \lesssim 0.007$), the distance between intercalated ethidiums is typically large and excitation transfer is negligible. In this case, only Brownian rotations of the initially excited dye subunit contribute to $\langle \Delta_z(t)^2 \rangle$ and $\langle \Delta_x(t)^2 \rangle$. In this case, the intermediate zone formula [42,43] applies, hence $\langle \Delta z(t)^2 \rangle = 2kT(\pi\alpha\gamma)^{-1/2} t^{1/2}$, and the corresponding twisting correlation function is

$$C_n(t) = \exp\left[-\frac{n^2 k_B T}{(\pi\alpha\gamma)^{1/2}} t^{1/2} \right], \qquad (8)$$

where α is the (adjustable) torsion constant between base-pairs, $\gamma = 6.15 \times 10^{-23}$ dyne-cm-s is the recently measured friction factor per base-pair for azimuthal rotation around the symmetry axis [44] and $k_B T$ is thermal energy. In this case, we also assume that $\langle \Delta_x(t)^2 \rangle = 0$, or $F_n(t) = 1.0$, which yields a lower bound for the best-fit α. If, instead, the Barkley–Zimm [42] formula for $\langle \Delta_x(t)^2 \rangle$ is employed with a bending rigidity corresponding to a persistence length $P = 500$ Å, the best fit α is increased by a factor of 1.9, which then provides an upper bound [4,6]. Evidence that the dynamic bending rigidity is actually about 3 times larger than that inferred from the corresponding static persistence length has been reported [6,45,46] (also personal communication from B.H. Robinson and E. Hustedt). When our current best estimate of the dynamic persistence length, $P = 1500$ Å, is employed, the best-fit α is increased above its lower bound by a factor of 1.35 [47]. Moreover, recent estimates of the static torsion constant obtained from the relative rates of circularization of small DNAs of different length [48] are now in good agreement with the best-fit α obtained from the FPA by using a dynamic persistence length $P = 1500$ Å [47]. Because the effect of intercalated dye on the dynamic persistence length is presently unknown, we continue to assume that the Brownian contribution to $\langle \Delta_x(t)^2 \rangle$ is vanishingly small, with the understanding that the best-fit α, though a lower bound, is proportional to α in any case and accurately reflects any changes in α.

When the binding ratio exceeds 1 dye per 50 bp ($r \geq 0.02$), the distance between some of the intercalated ethidiums is sufficiently small that excitation transfer makes a significant contribution to the rotational dynamics of the excitation frame. This will be demonstrated subsequently. The excitation transfer contribution must be superimposed on that due to Brownian rotations of the excitation frame. In fact, excitation transfer contributes in different ways to both $\langle \Delta_z(t)^2 \rangle$ and $\langle \Delta_x(t)^2 \rangle$, as detailed below.

Let $\eta(t)$ denote the angle between the initial direction of the transition dipole and its direction at time t. It is assumed for the moment that excitation transfer between intercalated ethidiums is the only process contributing to $\eta(t)$. Because transfer occurs between sites with discrete directions of their transitions dipoles, $\eta(t)$ is a discrete random variable rather than a continuous Gaussian random variable. Whatever the nature of $\eta(t)$, the exact contribution of that process to the FPA is $(2/5)\langle P_2 \cos \eta(t) \rangle$ [6,39]. The random excitation transfer between discrete sites along a straight rigid DNA is simulated using techniques developed by Genest et al. [14], as described in the next section. We now imagine an equivalent Gaussian random process for rotation around the symmetry axis of the excitation frame that produces the same FPA. Its mean

squared angular displacement ($\langle \delta_z(t)^2 \rangle$) is defined by the relation

$$\langle P_2 \cos \eta(t) \rangle = I_0 + I_1 E(t) + I_2 E(t)^4, \qquad (9)$$

where $E(t) = \exp(-\langle \delta_z(t)^2 \rangle / 2)$ [6]. The right-hand side of eq. (9) is valid only for a continuous Gaussian random process [39]. $E(t)$ is readily determined from $\langle P_2(\cos \eta(t)) \rangle$ by solving eq. (9) at each time point.

When the excitation transfer and Brownian contributions to rotation around the symmetry axis are superimposed, we obtain

$$\langle \Delta_z(t)^2 \rangle = 2k_B T (\pi \alpha \gamma)^{-1/2} t^{1/2} + \langle \delta_z(t)^2 \rangle.$$

It is implicitly assumed that, wherever the excitation instantaneously dwells, the Brownian dynamics of that dye-subunit, continues to follow the same trajectory in regard to $\langle \Delta_z(t)^2 \rangle$ and $\langle \Delta_x(t)^2 \rangle$ as the initially excited dye-subunit. In this event, the twisting correlation function becomes

$$C_n(t) = \exp\left[- \frac{n^2 k_B T}{(\pi \alpha \gamma)^{1/2}} t^{1/2} \right] E(t)^{n^2} \qquad (11)$$

If significant excitation transfer occurs, then $E(t) < 1.0$. This will cause a spurious decrease in the best-fit α, if $E(t)$ is omitted from the data analysis.

The helix along which excitation transfer takes place is normally bent, due to thermal fluctuations, rather than straight. As the excitation translates along a stationary bent DNA, the instantaneous excitation frame undergoes small (nearly continuous) rotations around its transverse x- and y-axes, besides the much larger angular jumps around its z-axis. The total translational displacement of the excitation is m base-pairs plus two half-dyes, equivalent to $m + 1$ base-pairs, and includes $m - 1 + 2 = m + 1$ bending springs. The chain of subunit symmetry axis vectors (called bond vectors) of the base-pairs and dyes is projected onto any plane containing the vector from the donor center to the acceptor center. In that plane (labelled the yz-plane), the mean-squared angular displacement of the bond vector of the acceptor dye with respect to that of the donor dye is $\langle \delta_{xm}^2 \rangle = |m + 1| \langle \theta^2 \rangle = |m + 1| h/P$ where $\langle \theta^2 \rangle = k_B T / \kappa_\beta$ is the mean-squared angle between the projection of any two consecutive bond vectors in the yz-plane, κ_β is the bending force constant for these springs, $h = 3.4$ Å is the rise per base-pair, and $P = h \kappa_\beta / k_B T$ is the persistence length [8,44]. Equation (12) applies only when $(m + 1)h$ is somewhat less than P. Thus translation along an equilibrium population of bent DNAs over m intervening base-pairs is equivalent to a mean-squared angular displacement $\langle \delta_{xm}^2 \rangle$ around the x-axis (or y-axis) of the excitation frame. The contribution of $\langle \delta_{xm}^2 \rangle$ to the tumbling correlation function with index n is $f_n(m) = \exp[-(6 - n^2) \langle \delta_{xm}^2 \rangle / 2]$. In the simulation of Genest et al. [14], the rms migration distance ($\langle r^2 \rangle^{1/2}$) at 80 ns is about 35 Å for $r = 0.20$. This distance corresponds to $m + 1 \cong 11$. Taking $P = 500$ Å and $m = 10$ in eq. (12) yields $\langle \delta_{x10}^2 \rangle = 0.075$, and $f_n(m) = 0.80$, 0.83, and 0.90 for $n = 0$, 1 and 2, respectively. This represents an appreciable relaxation of the tumbling correlation function and should not be neglected in the data analysis.

Simulation of the excitation transfer process yields the probability $P(m, t)$ that the excitation is displaced by m base-pairs at time t from the site of initial excitation at time 0. The mean squared angular displacements $\langle \delta_z(t)^2 \rangle$ and $\langle \delta_x(t)^2 \rangle$ at time t are obtained from averages over all configurations of bound dyes and all displacements of the excitation at time t. Thus,

$$\langle \delta_x(t)^2 \rangle = \sum_m P(m, t) \langle \delta_{xm}^2 \rangle, \qquad (13)$$

$$I_0 + I_1 E(t) + I_2 E(t)^4 = \sum_m P(m, t) P_2 \cos \eta_m \qquad (14)$$

where

$$\cos \eta_m = \cos^2 \epsilon_0 + \sin^2 \epsilon_0 \cos \delta_m \qquad (15)$$

is the angle between the transition dipoles of two intercalated ethidium molecules separated by m base-pairs in an undeformed DNA. δ_m is the azimuthal rotation angle between donor and acceptor (in degrees)

$$\delta_m = 36m - 26. \qquad (16)$$

It is assumed that the azimuthal succession angle between base-pairs along the helix is 36°. The tumbling correlation function due to excitation transfer (neglecting the Brownian dynamics) is

$$F_n(t) = \exp\left[-(6-n^2)\langle \delta x(t)^2\rangle/2\right] \qquad (17)$$

Of course, $F_n(t) < 1.0$ when excitation transfer is significant. This also will cause a spurious reduction in the best-fit α, if $\langle \delta_x(t)^2\rangle$ is omitted from the data analysis.

The present treatment differs from that of Genest and coworkers [11–14] in three main respects. (1) The anisotropy used here is given by eq. (4) with $C_n(t)$ from eq. (11) and $F_n(t)$ from eq. (17). The assumption of Genest and coworkers that $r(t)$ is a simple product of factors for Brownian motion and excitation transfer is evidently valid only when the Brownian motions are spherically symmetric, so $\langle \Delta_z(t)^2\rangle = \langle \Delta_x(t)^2\rangle$, and when the array of chromophores is spherically symmetric, i.e. $\langle \delta_z(t)^2\rangle = \langle \delta_x(t)^2\rangle$. The coupling between Brownian dynamics and excitation transfer is clearly somewhat more complicated for non-spherical molecules like DNA (2). The torsional dynamics of DNA is represented by the intermediate zone decay in eq. (8) rather than the simple exponential assumed by Genest and coworkers [2,6]. (3) The polar angle of ethidium is taken to be 70.5° [40,41] rather than 90°, as assumed by Genest and coworkers.

4. Simulation of excitation transfer

In treating each excitation transfer step, the DNA is assumed to be straight and untwisted. This is justified to some extent by the fact that single excitation transfers normally cover only rather short distances, over which deformation is typically negligible. However, after many such jumps, the rms translational displacement, $(m+1)h$, of the excitation may be rather large. Hence, bend of the intervening DNA must be considered in treating the emission polarization, as done above, though not in treating the excitation transfer *per se*. Twist of the intervening DNA is believed to exert a negligible effect on the emission polarization in this case, because the large azimuthal angular jumps accompanying excitation transfers are expected to overwhelm and average out such effects. The rate of transfer of an excitation from one base-pair to another separated by m base-pairs is given by [18]

$$k_m = \frac{A}{n^4 R_m^6}\left(\cos\,\eta_m - 3\cos^2\epsilon_0\right)^2, \qquad (18)$$

where $A = 1.77\times10^7$ ns^{-1} Å^6 is a constant [14] that contains the usual factors for overlap of the emission and absorption spectra and the radiative decay rate, $R_m = (m+1)h$ is the transfer distance, and n is the local refractive index. The value adopted, $n = 1.7$, is estimated from the refractive index increment and partial specific volume of DNA reported by Kam et al. [49]. It is close to the estimate ($n = 1.75$) proposed by Harrington [50].

A Monte Carlo algorithm devised by Genest et al. [14] is employed to randomly place the dyes along 1000 DNA chains, each containing 4000 bp, subject to nearest-neighbor exclusion, in such a way as to achieve (on the average) the experimental binding ratio r. The excitation begins on the dye closest to the center of the filament at $t = 0$. The random excitation transfer process is also simulated using a Monte Carlo algorithm developed by Genest et al. [14]. This algorithm admits excitation transfer to the two nearest neighboring ethidiums on either side of the currently excited ethidium. For each DNA chain, the trajectories of 100 different initial excitations are simulated. While calculating $\langle P_2\cos\eta(t)\rangle$ (the right-hand side of eq. (14)), we also calculate $\langle \delta_x(t)^2\rangle$ using eq. (13), and the mean squared translational displacement,

$$\langle R^2(t)\rangle = \sum_m \left((m+1)h\right)^2 P(m,t) \qquad (19)$$

5. Data analysis

Our general deconvolution and fitting protocol is described elsewhere [5,6]. Briefly, the sum data, $s(t) = i_{\parallel}(t) + i_{\perp}(t)$, are fitted to a convolution of

the instrument function with a theoretical sum function $S(t) = A_s(t) + S_1(t) + S_2(t)$, where the δ-function accounts for Raman scattered light from the solvent and $S_1(t)$ and $S_2(t)$ are exponential terms that account for emission from intercalated ($\tau_1 = 21 \pm 1$ ns) and free ($\tau_2 = 1.5$–2.5 ns) ethidium. The adjustable parameters are three amplitudes and two lifetimes. The difference data, $d(t) = i_\theta(t) - i_\perp(t)$, are fitted to a convolution of the instrument function with the theoretical difference function, $D(t) = r_s A_s \delta(t) + S_1(t) r_1(t) + S_2(t) r_2(t)$, where r_s is the anisotropy of the scattered light (typically 0.3), $r_1(t)$ is the anisotropy function for intercalated dye (i.e. $r_1(t) = r(t)$ in eq. 4), and $r_2(t)$ is the anisotropy function for free dye. In this work, the $S_2(t) r_2(t)$ term is negligible because $S_1(0)/S_2(0) \gtrsim 15$, and $r_2(t)$ relaxes in 85 ps [5], which is considerably less than the instrument function in this work (500 ps). All FPA data are fitted using eq. (4) in two ways. (1) Taking no account of excitation transfer. In this case, $C_n(t)$ is given by eq. (8), and $F_n(t) = 1.0$. (2) Taking account of excitation transfer. In this case, $C_n(t)$ is given by eq. (11) and $F_n(t)$ by eq. (17). $E(t)$ and $\langle \delta_x(t)^2 \rangle$ are obtained from the simulations at each time-point along the FPA decay curve and incorporated directly into $C_n(t)$ and $F_n(t)$. Otherwise the deconvolution and fitting procedure is the same as in the absence of excitation transfer.

The DLS photon correlation functions are fitted to a single-exponential plus baseline,

$$G^{(2)}(t) = A \exp(-t/\tau) + B, \tag{20}$$

where A, B and τ are adjustable parameters. The apparent diffusion coefficient is calculated from τ according to

$$D_{app}(K) = 1/2\tau K^2, \tag{21}$$

where the magnitude of the scattering vector is $K = (4\pi n_s/\lambda) \sin \theta/2$, θ is the scattering angle, λ is the wavelength of the incident beam *in vacuo*, and n_s is the refractive index of the solvent (1.334 at $\lambda = 632.8$ nm, 1.348 at $\lambda = 351.1$ nm). At large $K^2 = 20 \times 10^{10}$ cm^{-2}, $D_{app}(K) = D_{plat}$ reflects internal motions of the DNA over distances of 225 Å. Empirically, it is found for long linear DNAs that D_{plat} varies sensitivity and in parallel with the torsion constant determined from FPA, [9]. At its present stage of development, DLS theory provides only a qualitative understanding of this circumstance. In any case, D_{plat} measurements provide an independent criterion for validity of the excitation transfer simulations for linear DNA, as described below.

6. Results and discussion

Measured quantities here are generally reported as a function of added ethidium bromide per base-pair (EB/BP). Under conditions of these experiments, up to EB/BP = 0.20, the ethidium is practically all bound. This is inferred from eq. (3) using literature values for the equilibrium constant K and E_T summarized by Wu et al. [5], and is confirmed by the rather small relative amplitude of free dye fluorescence observed when EB/BP $\lesssim$ 0.20. Thus, in these studies it is a reasonable approximation to regard EB/BP as the binding ratio r up to EB/BP = 0.2.

Our FPA data are analyzed in two different ways, namely in the usual way taking no account of excitation transfer, and also taking account of excitation transfer by means of the simulations, as described above. Comparison of the results of these two methods provides a means to judge the effects of excitation transfer on the FPA dynamics.

6.1 Linear DNAs

The best-fit α values obtained for linear pBR322 DNA by accounting for excitation transfer, and also by taking no account of excitation transfer, are plotted vs. time-span of the data for EB/BP = 0.05 in Fig. 1. There is no evidence that intercalated ethidium introduces significant non-uniformity of the torsional rigidity. Clearly, excitation transfer acts to substantially decrease the apparent torsion constant when no account is taken of that process. Values of D_{plat} for linear pUC8 DNA are plotted vs. EB/BP in Fig. 2A. The torsion constants of linear pBR322 and pUC8 DNAs obtained by accounting for excitation

transfer, and also by taking no account of excitation transfer, are co-plotted in Fig. 2B. Clearly, D_{plat} remains constant, unaffected by ethidium binding up to EB/BP = 0.10. In fact, D_{plat} remains constant up to EB/BP = 0.20 (data point not shown in Fig. 2A). This implies rather strongly that the twisting rigidity of linear pUC8 DNA is not significantly affected by intercalated ethidium up to $r = 0.20$. Indeed, the torsion constants of linear pBR322 and pUC8 DNAs, obtained by accounting for excitation transfer, also remain constant (within the experimental errors), unaffected by intercalated ethidium up to $r = 0.10$. In contrast, the apparent torsion constants of linear pBR322 and pUC8 DNAs, obtained by taking no account of excitation transfer, are observed to decrease substantially over that same range. The parallel behavior of D_{plat} and α obtained by accounting for excitation transfer implies that the effects of excitation transfer have been reasonably accurately simulated. We conclude that the torsion constants of linear pBR322 and pUC8 DNAs are unaffected by intercalated ethidium up to a binding ratio $r = 0.20$ (1 dye per 5 bp). This is 40% of saturation binding in the nearest-neighbor exclusion model.

The effective torsion constant for the filament (α_{eff}) is related to that between two base-pairs

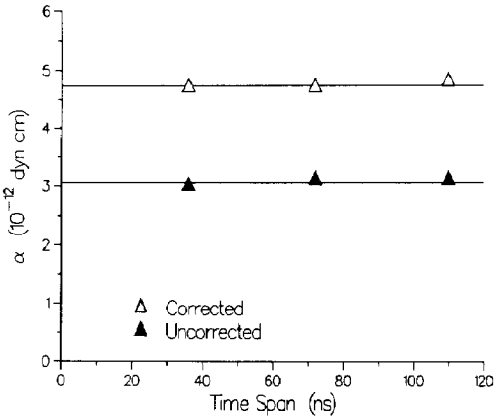

Fig. 1. Best-fit torsion constant α vs. time span of the data fitted for linear pBR322 DNA in 0.1 M NaCl, 10 mM EDTA, pH 8.0, $T = 20\,^{\circ}$C. (△) are α-values obtained after accounting for excitation transfer; (▲) are α-values obtained by taking no account of excitation transfer. The solid lines are located at the average α in each case.

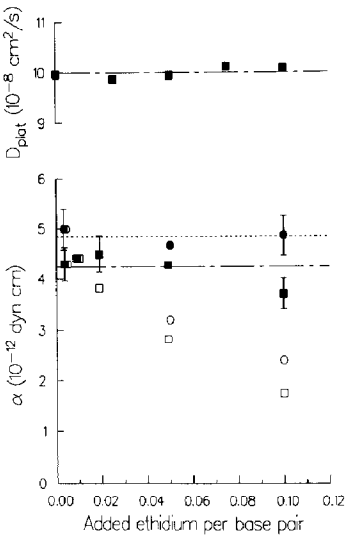

Fig. 2. A (Top) D_{plat} vs. added ethidium per base-pair ratio (EB/BP) for linear pUC8 DNA. A least-squares horizontal line is drawn through the experimental data (■). Standard deviations are comparable to the size of the symbols. Linear pUC8 DNA is in 0.1 M NaCl, 10 mM Tris, 10 mM EDTA, pH 8.0, $T = 20\,^{\circ}$C. B (Bottom) Torsion constant α of linear pUC8 (■) and pBR322 (●) DNAs vs. ethidium per base-pair ratio. Filled symbols are α-values obtained by accounting for excitation transfer (eqs. 11 and 17), while open symbols are α-values obtained by taking no account of excitation transfer (eq. (8) and $F_n(t) = 1.0$). Least-squares horizontal lines are drawn through each data set. Linear pBR322 DNA is in 0.1 M NaCl, 10 mM Tris, 1 mM EDTA, pH 8.5, $T = 20\,^{\circ}$C, and conditions for linear pUC8 DNA are as described above. When error bars are not displayed on the filled symbols, the standard deviations are comparable to the symbol size. Relative errors of the unfilled symbols are approximately the same as those of the corresponding filled symbols.

(α_0) and that between an intercalated ethidium and a base-pair (α_d) by [5]

$$\alpha_{eff} = \alpha_0 \frac{1}{(1-f) + f(\alpha_0/\alpha_d)} \qquad (22)$$

where f is the fraction of normal springs between base-pairs, and $1-f$ is the fraction of springs between intercalated ethidium and a base-pair. When $r = 0.20$, $f = 4/6$, $1-f = 2/6$. Our data indicate that α_{eff} (after accounting for excitation transfer) does not differ from α_0 by more than 15%, whence $0.85 \leq \alpha_{eff}/\alpha_0 \leq 1.15$. In conjunction with eq. (22), this indicates that $0.65 \leq \alpha_d/\alpha_0 \leq 1.64$. Thus, with some confidence we can say

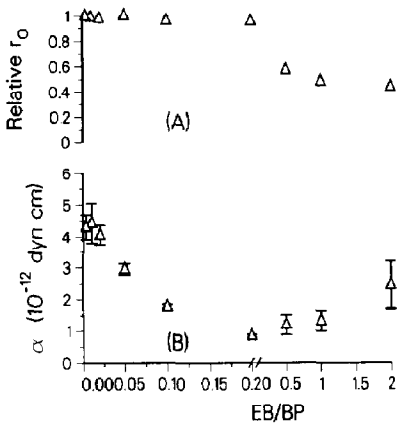

Fig. 3. Results obtained by taking no account of excitation transfer. Relative initial anisotropy (A) and apparent torsion constant (B) of linear pUC8 DNA vs. added ethidium per base-pair. Each point is the average of the values at three experimental time spans (36, 73 and 110 ns). The DNA is on 0.1 *M* NaCl, 10 m*M* Tris, 10 m*M* EDTA, pH 8.0, $T = 20\,^{\circ}$C.

that the torsion constant α_d between intercalated ethidium and a base-pair is not smaller than α_0 by more than 34% nor larger than α_0 by 65%, and is most probably nearly the same as α_0. In view of these limits, one may conclude that either (a) the ethidium intercalation sites in linear DNAs do not correspond to Sobell β-kinks, or (b) the torsion constant of a Sobell β-kink is not smaller than α_0 by as much as a factor of 2, and may not be smaller at all. These limits on α_d also rule out any greatly enhanced torsion constant between intercalated ethidium and its neighboring base-pairs. The hypothesis of Hogan and Jardetzky [51] that intercalated ethidium is rigidly clamped to its neighboring base-pairs is evidently not valid.

6.2 Results obtained by taking no account of excitation transfer

The effects of intercalated ethidium on the apparent torsion constant and relative initial anisotropy, obtained by taking no account of excitation transfer, are shown in Fig. 3. The apparent α remains constant from EB/BP = 0.0033 up to 0.010, then decreases from $\alpha \cong 4.5 \times 10^{-12}$ to $\alpha \cong 0.8 \times 10^{-12}$ dyne-cm as EB/BP increases from 0.010 up to 0.20. Over the range of EB/BP from 0.0033 up to 0.20 the initial anisotropy r_0 remains constant. As noted above the marked decrease in apparent α is entirely due to excitation transfer. Surprisingly, the apparent α is invariant to time-span of the experiment (0–36, 0–72, 0–120 ns) up to EB/BP = 0.20, despite a large contribution of excitation transfer. Apparently the contribution of excitation transfer to $\langle \delta_z(t)^2 \rangle$ and $\langle \delta_x(t)^2 \rangle$ produces an FPA decay similar to that induced by the Brownian dynamics.

As EB/BP increases further from 0.2 to 2.0, the apparent α increases by about 2-fold and r_0 decreases by about 2-fold. A probable explanation for this decrease in r_0 is that excitation transfer causes some very rapid depolarization on a time-scale too short to resolve, when EB/BP $\geq$ 0.50. Any process too rapid to resolve acts to reduce r_0. This initial depolarization due to rapid excitation transfer is predominantly azimuthal rather than polar (i.e. $\langle \delta_z(t)^2 \rangle \gg \langle \delta_x(t)^2 \rangle$), so all three terms in $r(t)$ (in eq. 4) are not reduced by the same initial anisotropy factor, $r_0/0.4$. Instead the $n = 2$ term experiences a greater relative decrease in amplitude than the $n = 1$ term, which in turn experiences a considerably greater relative decrease than the $n = 0$ term. Thus, in the resolved part of the decay, the slower components gain relative amplitude at the expense of the faster components. Consequently, when the same r_0 is assumed to apply for all three terms, the apparent torsion constant will be substantially increased for EB/BP $\geq$ 0.50, as observed. A quantitative analysis of this increase in apparent α and decrease in r_0 for EB/BP $\geq$ 0.50 has not yet been accomplished, so it would be premature to conclude that no other factors, such as structural changes in the DNA, contribute to the rise in apparent α. Subsequent discussion is confined to the range $0.0033 \leq$ EB/BP ≤ 0.10, where there is no evidence for any effect of rapid excitation transfers on the initial anisotropy r_0.

6.3 Excitation transfer

The rate of Förster-type transfer is sensitive to both the separation and relative orientation of the donor–acceptor pair. To the extent that the separations and relative orientations of interca-

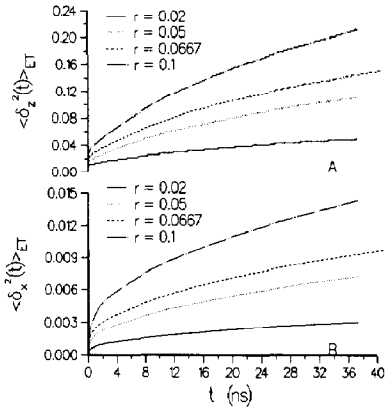

Fig. 4. Effect of excitation transfer on motion of the excitation frame. Mean-squared angular displacement around the helix-axis (A) and around a transverse axis (B) vs. time at four binding ratios. From top to bottom: $r = 0.1$, 0.0667, 0.05 and 0.02.

lated ethidiums in DNA are fairly well defined, DNA/ethidium complexes provide a useful substrate for testing Förster theory in regard to identical chromophores. The simulation procedure used here is based on a random distribution of intercalated dyes among the available sites, employs standard geometrical parameters for the DNA, invokes a plausible value of the local refractive index, and produces excitation transfers with an average rate given by the Förster formula. Up to $r = 0.10$ (or EB/BP = 0.10), this simulation protocol is substantially validated by the parallel behavior of D_{plat} and α obtained by accounting for excitation transfer. This implies that Förster theory provides an adequate account of most of the excitation transfers that take place in DNA/ethidium complexes at least up to $r = 0.10$.

The simulated contributions of excitation transfer to $\langle \delta_z(t)^2 \rangle$ and $\langle \delta_x(t)^2 \rangle$ are displayed for various binding ratios r (or EB/BP) in Fig. 4. The mean squared angular displacement ($\langle \delta_z(t)^2 \rangle$) of the equivalent Gaussian random process for rotation of the excitation frame around its z-axis exceeds the mean-squared angular displacement ($\langle \delta_x(t)^2 \rangle$) for rotation around a transverse axis by more than an order of magnitude. The corresponding mean squared linear displacements of the excitation along the chain are presented elsewhere [52]. For $r = 0.10$, the rms linear displacement ($\langle R(t)^2 \rangle^{1/2}$) is 5 Å at 1 ns, 8.7 Å at 10 ns, and 13.4 Å at 40 ns. The corresponding root mean square angular displacements of the excitation frame around its z-axis ($\langle \delta_z(t)^2 \rangle^{1/2}$) are 11.5° at 1 ns, 18.3° at 10 ns, and 25.6° at 40 ns. The corresponding rms angular displacements of the excitation frame around a transverse axis ($\langle \delta_x(t)^{1/2} \rangle$) are 3.6° at 1 ns, 5.1° at 10 ns, and 6.8° at 40 ns. For comparison, the Brownian contributions to $\langle \Delta z(t)^2 \rangle^{1/2}$ (obtained from the prelude to eq. 8) can be estimated for $\alpha = 4.5 \times 10^{-12}$ and $\gamma = 6.15 \times 10^{-23}$ to be 16.9° for 1 ns, 30° for 10 ns, and 42° for 40 ns. Thus, when $r = 0.10$, the contribution of excitation transfer to rms rotation of the transition dipole around the symmetry axis is about 2/3 that of the Brownian twisting deformations over the range 1 to 40 ns.

6.4 Supercoiled DNAs

The torsion constants of supercoiled pBR322 and pJMSI1 DNAs obtained by accounting for excitation transfer, and also by taking no account of excitation transfer, are plotted vs. EB/BP in Fig. 5. As expected, α decreases with increasing EB/BP, when no account is taken of excitation transfer. But even after accounting for excitation transfer, α still decreases substantially with increasing EB/BP! The effect of intercalated ethidium to reduce the torsion constant of supercoiled, but not linear, DNAs is similar to what was observed for intercalated chloroquine in the same buffer. However, ethidium causes an appreciably larger decrease in α for any given r. The superhelix density of these DNAs is completely relaxed at EB/BP $\cong r^* = 0.064$. At $r^* = 0.064$, the extrapolated α of the supercoiled pBR322 DNA/ethidium complexes is about 3.3×10^{-12} dyne-cm, while that of the linear pBR322 DNA/ethidium complexes is about 4.8×10^{-12} dyne-cm. This discrepancy amounts to 31% of the latter value. At the r^* where chloroquine completely relaxes supercoiled pBR322 DNA, the corresponding discrepancy is about 15% [5].

Significant differences in the responses of these linear and supercoiled DNAs to increasing

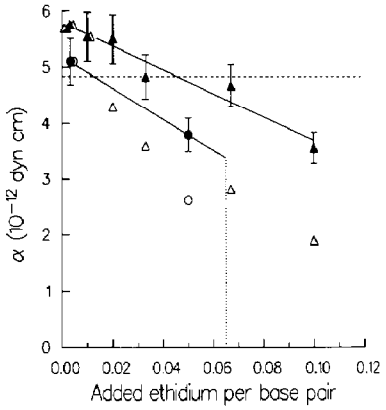

Fig. 5. Torsion constant α of supercoiled pBR322 (●) and pJMSII (▲) DNAs vs. ethidium per base-pair ratio. Filled symbols are α-values obtained by taking account of excitation transfer (eqs. 11 and 17), while open symbols are α-values obtained by taking no account of excitation transfer (eq. 8 and $F_n(t) = 1.0$). The two continuous dark lines are least-squares fits to the respective data sets. The dashed line is the best-fit horizontal line for linear pBR322 from Fig. 2. The vertical dotted line denotes the ethidium per base-pair ratio at which $r = r^* = 0.065$ and both supercoiled DNAs are completely relaxed. Buffer conditions for supercoiled pBR322 DNA are the same as for its corresponding linear pBR322 DNA in Fig. 2. Supercoiled pJMSII DNA is in 0.1 *M* NaCl, 10 m*M* Tris, 1 m*M* EDTA, pH 8.0, $T = 20\,^{\circ}$C. When error bars are not displayed on the filled symbols, the standard deviations are comparable to the symbol size. Relative errors of the unfilled symbols are approximately the same as those of the corresponding filled symbols.

EB/BP are observed even when excitation transfer is not taken into account. In fact, when EB/BP = 0.050, the ratio of the torsion constants of linear and supercoiled pBR322 DNAs is virtually the same whether or not excitation transfer is taken into account (1.24 vs. 1.23). The *difference* between the *overall decrease* in torsion constant of supercoiled pBR322 DNA and that of linear pBR322 DNA, as EB/BP varies from 0.003 to 0.050, is comparable whether or not excitation transfer is taken into account—(0.9 vs 0.6) $\times$ 10^{-12} dyne-cm. Either way, the difference in decreases amounts to nearly 3 standard deviations of the measured values. Likewise, the difference between the overall decrease in torsion constant of supercoiled pJMSII DNA and that of linear pUC8 DNA, as EB/BP varies from 0.003 to 0.10, is comparable, whether or not excitation transfer is taken into account—(1.6 vs. 1.3) $\times$ 10^{-12} dyne/cm. Either way, this amounts to nearly 4 standard deviations of the measured values. In this sense, the different responses of the linear and supercoiled DNAs to increasing EB/BP are manifested to a comparable and significant extent in either data set, and cannot be attributed to any artifact arising from the protocol for taking excitation transfer into account.

Another comparison between the effects of ethidium and chloroquine concerns the twist energy parameters inferred from dye-binding data. Both dyes typically yield substantially lower (by two-fold or more) E_T values than are obtained by analysis of relaxed topoisomer distributions and, of the two, ethidium yields the smaller values, which are about 75% of those obtained with chloroquine [5]. The observed reductions in the torsion constants of supercoiled DNAs by both dyes (in 0.1 *M* NaCl) are qualitatively consistent with lower E_T values, but are too small to account quantitatively for such large reductions in E_T. Likewise, the smaller torsion constants observed for supercoiled DNA/ethidium complexes compared to DNA/chloroquine complexes are qualitatively consistent with the lower E_T values of the former compared to the latter, but again a quantitative correspondence is lacking.

There are three important aspects to the present comparison of supercoiled and linear DNAs.

(1) At $r = 0$, the (extrapolated) torsion constant of native supercoiled pBR322 DNA slightly exceeds that of its corresponding linear DNA, as found also in a previous study. Although this small difference does not exceed the combined statistical errors of the two measurements, its consistency for several different sample pairs suggests that it is probably real. In the case of pUC8 DNA, a slightly larger torsion constant is also observed for the native supercoiled form than for either the linear or fully relaxed supercoiled species [53]. In the case of M13mp7 DNA (at lower salt concentration), a significantly larger torsion constant is observed for the supercoiled form than for the linear species [4,53]. Such enhancement of the torsion constants of native supercoiled DNAs, though small in the case of

pBR322 and pUC8 plasmids, might be a general phenomenon. However, this observation cannot account even qualitatively for the reported failures of eqs. (2) and (3) at intermediate and native superhelix densities, because those would require a *significantly smaller* torsion constant of the native supercoiled DNA. However, a slightly enhanced torsion constant would be consistent with the possibility that a different equilibrium secondary structure with greater torsional rigidity prevails over at least some of the the sequence in the native supercoiled DNA, as suggested previously [4–6,53,54].

(2) The torsion constants of the linear DNAs remain unaffected by intercalated ethidium up to $r \sim 0.20$, whereas those of the native supercoiled DNAs decrease substantially over the observed range of r. Evidently, linear DNAs exhibit the invariance of torsion constant to bound ethidium that was assumed in the derivation of eq. (3), but native supercoiled DNAs exhibit a rather different response, namely a progressive decrease in torsion constant with increasing binding ratio up into the region of positive supercoiling $r > r^* = 0.064$. This apparent decrease in torsion constant of the native supercoiled form must be attributed to either (I) a real decrease in torsion constant, or (II) clustering of the dye in the supercoiled DNA, possibly in a condensed domain of tertiary structure, with concomitant depolarization by excitation transfer. The latter possibility is discounted, because a decrease in apparent torsion constant is also induced by chloroquine, which does not transfer excitation to ethidium. Also, dye clustering would be reflected in enhanced binding affinity, but the actual affinity of native supercoiled pBR322 DNA for ethidium is less than expected; indeed that is the origin of the low E_T value. A real decrease in torsion constant could be due to either (i) a direct effect of intercalated ethidium to reduce the torsion constant of the prevailing secondary structure, or (ii) an indirect effect of the dye to increase the superhelix density (i.e. decrease the superhelical stress) coupled with a generic decrease in torsion constant with increasing superhelix density over this range, or some combination of both. Either possibility would be consistent with the prevalence of a different equilibrium secondary structure over at least some of the sequence in the native supercoiled DNA, as suggested before [53].

(3) At EB/BP $\cong r^* = 0.064$, where the superhelix density and superhelical stress vanish, the extrapolated torsion constant of the fully relaxed supercoiled pBR322 DNA/ethidium complexes lies significantly below that of the corresponding linear pBR322 DNA/ethidium complexes. As noted in Section 1.3.1, these particular DNAs with $r = r^*$ must coexist with the same concentration of free dye, have the same distribution of bound dye, and exhibit the same torsion and bending constants, provided that their tertiary structures remain uncondensed and that their secondary structures are both at equilibrium.

It is most unlikely that the observed discrepancy in torsion constants is due to any intramolecular condensation of the DNA/dye complexes with $r = r^*$ for the following reasons, in addition to those noted above. Binding data typically follow eq. (3) rather closely with no evidence of any cooperativity, which would be expected to accompany intramolecular condensation [5,33–35]. Hydrodynamic measurements, including sedimentation [15,55,56], diffusion [57], viscosity [58], and flow dichroism [59] indicate that the hydrodynamic radius of the supercoiled DNA actually increases with increasing bound dye toward a maximum at $r = r^*$. Moreover, the hydrodynamic radius at the maximum is nearly identical to that of the corresponding nicked circular DNA/dye complex with $r = r^*$ [55]. The hydrodynamic radius of that nicked circular DNA varies only slightly, smoothly, and nearly linearly with r from 0 up to $r > r^*$, and shows no sign of any intramolecular condensation. One may infer that the hydrodynamic radius of the supercoiled DNA with $r = r^*$ is nearly the same as that of its uncondensed nicked circular DNA. If we discount the possibility of intramolecular condensation, then any difference in torsion constant between the linear and fully relaxed supercoiled DNA/dye complexes with $r = r^*$ must be ascribed to non-equilibrium secondary structure in one or both species. The truth of this statement can readily be seen as follows. The same final state can be achieved by either of two routes,

namely (i) relaxing the native supercoiled DNA to $\sigma = 0$ by adding ethidium until $r = r^*$, or (ii) adding ethidium to linear DNA until $r = r^*$ and then ligating the linear complexes to form circles. Simple circularization of long DNAs is *not* expected to significantly alter the binding ratio, secondary structure, twisting or bending rigidity, or the FPA dynamics, provided intramolecular condensation does not occur [36]. Hence the circular species obtained by either route should exhibit the same FPA dynamics as the linear DNA, provided they are at equilibrium. The observed discrepancy between the torsion constants of the relaxed supercoiled and linear pBR322 DNAs with $r = r^*$ thus implies the existence of some incompletely equilibrated, or metastable, secondary structure in either the supercoiled or linear species, or both. We believe that the torsion constants of the relaxed supercoiled and linear DNA/ethidium complexes with $r = r^*$ must approach a common value at sufficiently long time, which evidently exceeds 1 month. Evidence for equilibration times of a month or more following linearization of supercoiled pBR322, pUC8, and M13 mp7 DNAs, or following partial relaxation (by Topoisomerase I) of supercoiled pUC8 dimer DNAs, was presented previously [53]. The molar ellipticity at 273 nm following linearization of p30δ DNA also evolves over time in a similar manner as found for the torsion constants of the other linearized plasmid DNAs (J. Delrow, P. Heath, J. Gebe, D. Stewart, and J.M. Schurr, 1990, unpublished results).

Metastable secondary structure, as evidenced by the unequal torsion constants of relaxed supercoiled and linear DNAs with $r = r^*$, has now been observed using several different intercalators, namely ethidium, chloroquine [5,20] 9-aminoacridine, and proflavine [52,54], and appears to be a common phenomenon. Additional evidence for metastable structure in dye-relaxed supercoiled DNAs comes from gel electrophoresis studies [27,64]. Differences in electrophoretic mobility between dye-relaxed supercoiled topoisomers with $\sigma = 0$ and nicked circular DNAs in gels containing ethidium, proflavine, 9-aminoacridine, quinacrine, or daunomycin, are also ascribed to metastable secondary structure in one or both species [53]. It is reasonable to suppose that the same metastable secondary structure is responsible for the differences in regard to both torsion constant and electrophoretic mobility between the relaxed supercoiled DNA and either the linear or nicked circular DNA with $r = r^*$. This metastable structure evidently responds differently to intercalated ethidium than does the normal B-helix of an equilibrium linear DNA. Another indication of this rather different response comes from flow dichroism studies [59]. The flow dichroism of supercoiled ϕX-174, SV40, and pBR322 DNA/ethidium complexes observed at 520 nm varies with ethidium concentration in a very different manner from that observed at 260 nm [59]. In particular the expected maximum in the absolute dichroism near $r = r^*$ is observed at 260 nm, where the bases absorb, but not at 520 nm, where only the ethidium absorbs. In contrast, for linear DNAs, the absolute flow dichroism at 520 nm closely parallels that at 260 nm, which increases slightly with increasing ethidium. These observations imply that ethidium is either bound to regions of the supercoiled DNA with peculiar properties, or induces (or traps) peculiar properties wherever it binds.

The present experiments do not unequivocally establish whether the metastable secondary structure prevailing at $r = r^*$ resides primarily in the supercoiled or in the linear species. The changes in torsion constant and, by inference, in the secondary structure of the supercoiled DNA with increasing intercalated ethidium mark it as the most likely candidate to undergo an incomplete change in secondary structure. Direct evidence for the existence of metastable secondary structure in freshly relaxed (by Topoisomerase I) or linearized supercoiled DNAs indicates that such metastable secondary structure is associated with the recent release of superhelical stress [53]. The common belief that the global secondary structure of supercoiled DNAs always converts immediately to unstrained (or less strained) B-helix upon complete (or partial) relaxation of the superhelix density evidently does not correspond to the facts. In view of these considerations, we presume that the metastable secondary structure in the present experiments resides primarily in

the more recently relaxed (by dye) supercoiled DNAs.

6.5 Implications of the metastable secondary structure

Before discussing the metastable structure, it is useful to classify the strains induced by superhelical stress. Local strains (e.g. local torsion or bending between base-pairs, base-tilt, base-roll, etc.) induced by superhelical stress are defined with respect to a reference state, namely the unstrained linear DNA. The secondary structure of this reference state will be referred to as unstrained B-helix, or simply B-helix, even though it may exhibit significant sequence-dependent variations, such as permanent bends, along the DNA. We distinguish simple strains from more general kinds of strain. A local strain is classified as simple when its free-energy increases monotonically with increasing mean displacement of each strain coordinate from its reference value. There are no yield points within the domain where the local strain remains simple. When the local strain proceeds beyond a yield point, the strain free energy declines (spontaneously) with further displacement into a secondary minimum associated with an alternate secondary structure.

The metastable secondary structure that apparently exists in freshly relaxed supercoiled DNAs is significant, because it represents a non-simple strained state, in which one or more strain coordinates are hindered by free-energy barriers from evolving to their equilibrium B-helix values. This metastable secondary structure must originate from a parent state that is presumably at equilibrium under native superhelical stress, and which likewise is non-simply strained (otherwise it would not give rise to a metastable state upon release of the superhelical stress). It can be inferred that native superhelical stress, or superhelix density, induces at equilibrium an alternative structure, namely the parent state, that is not derived by simple strains from unstrained B-helix. In other words, the existence of metastable secondary structure in freshly relaxed supercoiled DNA necessarily implies that one or more transitions in equilibrium secondary structure are induced when the superhelix density is varied from $\sigma = -0.05$ or 0 or vice-versa. The existence of a metastable state can be taken as firm, if indirect, evidence that an intensive variable (e.g. superhelix density) has just traversed the midpoint(s) of one or more structural transitions.

6.6 Extent of the alternate secondary structure

The question now is whether the persistent metastable state arises from one or more alternate global secondary structures that may prevail in supercoiled DNAs [6,53,54,60], or from one or a few radical structures of small extent, such as cruciforms, amidst a global, simply strained, B-type secondary structure. The latter possibility seems unlikely for several reasons. At $r^* = 0.064$, where the supercoiled DNAs are completely relaxed, the number of bound ethidiums per plasmid is 280. In order to affect the FPA, a majority, or at least a substantial fraction, of these ethidiums would have to bind at or near the sites of the one or a few radical structures of small extent. Such a non-uniform distribution of bound dye requires preferentially higher binding affinity for those sites. If that were the case, then the effective binding constants for supercoiled DNAs at low binding ratios would have to be anomalously large. To the contrary, competitive dialysis measurements show that the effective binding constant for ethidium at low r values is actually smaller than expected; that is origin of the low E_T values [5]. Any effect of one or a few radial structures of small extent to decrease the torsional rigidity would also be expected to yield non-uniform best-fit torsion constants over the different time-spans analyzed, contrary to observation [5,20]. Migration of the supercoiled topoisomers with $\sigma = 0$ well ahead of the nicked circular band in gels containing ethidium (or the other dyes noted above) also cannot be simply ascribed to one or a few radical structures of small extent. Any effect of only one or a few such structural anomalies on the agarose gel mobilities of relaxed plasmid DNAs should be entirely negligible. It is more likely that the metastable state arises from one or more alternate secondary structures of considerable, if not global, extent

that exhibit different torsional and bending rigidities.

It is conceivable that the distribution of intercalated ethidium is substantially more non-uniform is supercoiled than in linear DNA. Clustering of the intercalated ethidium into one region of the supercoiled DNA would certainly thwart out attempt to account for excitation transfer, and would yield anomalously low apparent torsion constants due to the enhanced excitation transfer. At $r = 0.10$ the number of bound dyes is so large (436) that the smallest cluster domain, subject to nearest neighbor exclusion, is nearly 900 bp. Hence, this possibility too would require an extended domain of altered secondary structure with relatively higher affinity for the dye. The relative affinity of supercoiled pBR322 DNA for ethidium is considerably lower than expected [5], hence any clustering would have to be attributed to one or more domains of secondary structure with rather low affinity for ethidium (compared to linear DNA) interspersed with one or more domains of higher affinity.

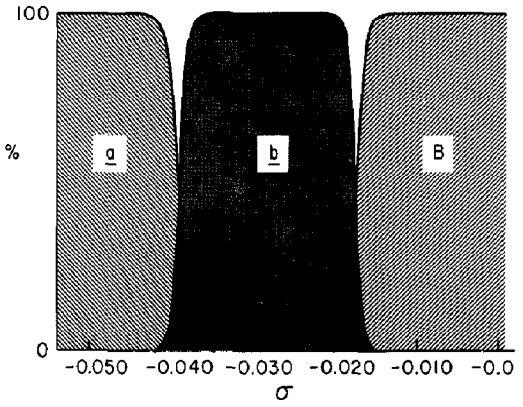

Fig. 6. Proposed intramolecular "phase diagram" for % of various global secondary structure types as a function of superhelix density σ. This highly idealized conjecture is based on data from dynamic light scattering, fluorescence polarization anisotropy and circular dichroism studies on pUC8 dimer [12,14]. What fraction of the DNA sequence may actually conform to this diagram is not known. The proposed states a and b represent distinct new secondary structures that are more stable than simply strained B-helix for $-0.05 \leq \sigma \leq -0.018$. The state b exhibits a low torsion constant. The proposed diagram is intended to apply only for 0.1 *M* NaCl, 10 m*M* Tris, 1 m*M* EDTA, pH 8.0, $T = 20$ to 21°C. Evidence that the b state may be favored by citrate or cacodylate buffers has been reported [11].

6.7 A tentative explanation

We propose the following tentative model, which is based on studies of supercoiled pUC8 dimer DNA as a function of superhelix density [53].

(1) At least two alternate global secondary structures can prevail over much or all of the sequence in supercoiled DNAs, as indicated schematically in Fig. 6. One alternate structure (called a) exhibits a torsion constant slightly higher than that of the equilibrium linear DNA, and is the stable form at native superhelix density ($\sigma = -0.05$) in Tris buffer [53,60]. The other alternate structure (called b) exhibits a substantially lower torsion constant and perhaps also a different bending rigidity, a significantly different circular dichroism, and is stable at intermediate superhelix density ($-0.033 \geq \sigma \geq -0.020$) in Tris buffer [53]. It also appears to be favored by citrate and cacodylate buffers [60]. Direct evidence consistent with this hypothesis has been reported [6,53,54,60,61].

(2) As the superhelix density is diminished from its native value, $\sigma = -0.050$, toward $\sigma = 0$, the secondary structure would be expected to undergo two successive transitions, first from a to b near $\sigma = -0.037$, and then from b to B near $\sigma = -0.018$ [53,54]. These transition regions are indicated in Fig. 6. However, the second transition, especially, is not kinetically facile, and proceeds at an extremely slow rate for at least some of the total sequence. Consequently DNAs that are relaxed to superhelix densities below $\sigma = -0.018$ may be trapped for an extended time in the metastable secondary structure b with anomalously low torsion constant. Thus metastable b structure with low torsion constant may occur commonly, regardless of whether the superhelix density is relaxed by linearization [53,54,60], by Topoisomerase I, [53,62], by intercalated chloroquine [5,20] or ethidium [6] or by *E. coli* single strand binding protein [63]. Furthermore, intercalating dyes may act to promote or induce the

metastable b state. These two hypotheses may provide a basis for understanding not only the present observations, but also the reported failures of eqs. (2) and (3), and the surprising flow dichroism data [59].

(1′) The occurrence of extensive transitions in secondary structure would cause the free-energy of supercoiling to rise less rapidly than the expected quadratic increase with linking difference (or superhelix density), as reported [31,32].

(2′) E_T obtained from dye-binding data via eq. (3) may be considerably smaller than that obtained by analysis of nearly relaxed topoisomer distributions using eq. (2) for three reasons. First, some of the DNA may be trapped in the b state with lower torsion constant, and perhaps also lower bending rigidity, for which E_T actually is lower. Second, the free energy difference between the a structure that prevails at $\sigma = -0.050$ and B-helix at $\sigma = 0$ is not as great as that between strained B-helix at $\sigma = -0.050$ and B-helix at $\sigma = 0$, so supercoiling does not enhance the dye-binding at much as predicted from the properties of B-helix alone. Third, not all of the free-energy difference between the a structure at $\sigma = -0.05$ and B-helix at $\sigma = 0$ may be realized, because part or all of the relaxed DNA may be trapped in the metastable b state, which has a higher free-energy than B-helix for $-0.018 \leq \sigma$.

(3′) Relaxation of supercoiled DNAs by ethidium and other intercalators may normally result in extended trapping or induction of the metastable b state with low torsion constant, as observed. In such an event, the b to B transition will be inhibited. Interestingly, the torsion constant continues to decrease with increasing ethidium beyond the point where $\alpha = -0.018$. Possibly sufficient ethidium shifts the transition to more positive σ values by actually preferring and inducing the intermediate structure b.

(4′) Both the enhanced electrophoretic mobility (relative to nicked circles) of the $\sigma = 0$ topoisomer and coalescence of the nearly relaxed topoisomer bands in the presence of ethidium [64] (and other intercalators) may reflect properties of the metastable b state. A significantly lower ratio of torsion constant to bending constant in that state would facilitate the absorption of writhe into twist and produce a concomitant loss of resolution. The mobility difference between the topoisomer with $\sigma = 0$ and nicked circles is presumably due to a different bending rigidity of the metastable b state in the supercoiled species.

(5′) The orientation of intercalated ethidium in the intermediate b state may well differ significantly from that in the a and B states [53]. If also ethidium preferentially intercalates in the b state and progressively enlarges its domain of stability, as suggested above, then the extent of the b state may increase with increasing ethidium, even when $-0.018 < \sigma \leq 0$. In such a case the flow dichroism of intercalated ethidium should exhibit a rather different variation with EB/BP than that of the bases themselves, as observed [59].

We emphasize that these hypotheses are tentative. Their value lies in the fact that they account for several rather unexpected observations, and do not conflict with any of the broad array of pertinent experimental observations, so far as we are aware, and they are testable in various ways.

If this proposed explanation is valid, three questions come immediately to mind. (i) What are the alternate a and b structures? Why are the kinetics of the b to B transition so slow? (iii) Of what significance is this for biology? These same questions are addressed elsewhere [53], and the interested reader is referred to that work.

Acknowledgement

This work was supported in part by grant R01-GM29338 from the National Institutes of Health (supercoiled DNAs) and grant DMB-8703467 from the National Science Foundation (linear DNAs).

References

1 H.M. Sobell, T.D. Sakore, J.A. Banerjee, K.K. Bhanclary, B.S. Reddy and E.D. Lozansky, Cold Spring Harbor Symp. Quant. Biol. 47 (1983) 273–314.

2 J.C. Thomas, S.A. Allison, C.J. Appellof and J.M. Schurr, Biophys. Chem. 12 (1980) 177–188.

3 J.C. Thomas and J.M. Schurr, Biochemistry 22 (1983) 6194–6198.
4 J.H. Shibata, B.S. Fujimoto and J.M. Schurr, Biopolymers 24 (1985) 1909–1930.
5 P.-G. Wu, L. Song, J.B. Clendenning, B.S. Fujimoto, A.S. Benight and J.M. Schurr, Biochemistry 27 (1988) 8128–8144.
6 J.M. Schurr, B.S. Fujimoto, P.-G. Wu and L. Song, Fluorescence studies of nucleic acids. Dynamics, rigidities, and structures, in: Fluorescence spectroscopy, ed. J.R. Lakowicz (Plenum, New York, NY, 1991).
7 J.C. Thomas, S.A. Allison, J.M. Schurr and R.D. Holder, Biopolymers 19 (1980) 1451–1474.
8 J. Wilcoxon and J.M. Schurr, Biopolymers 22 (1983) 2273–2321.
9 J.M. Schurr and K.S. Schmitz, Annu. Rev. Phys. Chem. 37 (1986) 271–305.
10 J. Paoletti and J.B. LePecq, J. Mol. Biol. 59 (1971) 43–62.
11 D. Genest and Ph. Wahl, Biochim. Biophys. Acta 259 (1972) 175–188.
12 D. Genest and Ph. Wahl, Biophys. Chem. 7 (1978) 317–323.
13 D. Genest and Ph. Wahl, in: Time resolved fluorescence spectroscopy in biochemistry and biology, eds. R.B. Cundall and R.E. Dale (Plenum, New York, NY, 1983) pp. 523–539.
14 D. Genest, P. Wahl and J.C. Auchet, Biophys Chem. 1 (1974) 266–278.
15 W. Bauer, Annu. Rev. Biophys. Bioeng. 7 (1978) 287–313.
16 J.C. Wang, J. Mol. Biol. 89 (1974) 783–801.
17 D.E. Pulleyblank and A.R. Morgan, J. Mol. Biol. 91 (1975) 1–13.
18 Th. Förster, Disc. Faraday Soc. 27 (1959) 7–17.
19 M. LeBret, J.B. LePecq, J. Barbet and B.P. Roques, Nucleic Acids Res. 4 (1977) 1361–1378.
20 P.-G. Wu and J.M. Schurr, Biopolymers 28 (1989) 1695–1703.
21 F.B. Fuller, Proc. Natl. Acad. Sci. USA 68 (1971) 815–819.
22 J.H. White, Am. J. Math. 91 (1969) 693–728.
23 J. Shimada and H. Yamakawa, J. Mol. Biol. 184 (1985) 319–329.
24 A.V. Vologodskii, V.V. Anshelevich, A.V. Lukashin and M.D. Frank-Kamenetskii, Nature (London) 280 (1979) 294–298.
25 M. LeBret, Biopolymers 19 (1980) 619–637.
26 Y. Chen, J. Chem. Phys. 75 (1981) 2447–2453.
27 D.E. Pulleyblank, M. Shure, D. Tang, J. Vinograd and H.P. Vosberg, Proc. Natl. Acad. Sci. USA 72 (1975) 4280–4284.
28 R.E. Depew and J.C. Wang, Proc. Natl. Acad. Sci. USA 72 (1975) 4275–4279.
29 D. Shore and R.L. Baldwin, J. Mol. Biol. 170 (1983) 957–1007.
30 D. Horowitz and J.C. Wang, J. Mol. Biol. 173 (1984) 75–91.
31 C.J. Benham, Cell Biophysics 10 (1987) 193–204.
32 S.A. Kozyavkin, A.I. Slesarev, S.R. Malkhosyan and I.G. Panyutin, Eur. J. Biochem. 191 (1990) 105–113.
33 W. Bauer and J. Vinograd, J. Mol. Biol. 47 (1970) 419–435.
34 T.S. Hsieh and J.C. Wang, Biochemistry 14 (1975) 527–535.
35 D.M. Hinton and V.C. Bode, J. Biol. Chem. 250 (1975) 1061–1079.
36 J. Langowski, B.S. Fujimoto, D.E. Wemmer, A.S. Benight, G. Drobny, J.H. Shibata and J.M. Schurr, Biopolymers 24 (1985) 1023–1056.
37 A.S. Benight, J. Langowski, P.-G. Wu, J. Wilcoxon, J.H. Shibata, B.S. Fujimoto, N.S. Ribeiro and J.M. Schurr, in: Laser scattering spectroscopy of biological objects, eds. J. Stepanek, P. Anzenbacher and B. Sedlacek (Elsevier, Amsterdam, 1987) pp. 407–422.
38 A.S. Benight, N.S. Ribeiro, L. Song, B.S. Fujimoto, P.-G. Wu, J.B. Clendenning and J.M. Schurr, Biophys. J. 51, (1987) 422a.
39 J.M. Schurr, Chem. Phys. 84 (1984) 71–96.
40 J.M. Schurr and B.S. Fujimoto, Biopolymers 27 (1988) 1543–1569.
41 M.E. Hogan, N. Dattagupta and D.M. Crothers, Biochemistry 18 (1979) 280–288.
42 M.D. Barkley and B.H. Zimm, J. Chem. Phys. 70 (1979) 2991–3007.
43 S.A. Allison and J.M. Schurr, Chem. Phys. 41 (1979) 35–59.
44 P.-G. Wu, B.S. Fujimoto and J.M. Schurr, Biopolymers 26 (1987) 1463–1488.
45 S.A. Allison, R.H. Austin and M.E. Hogan, J. Chem. Phys. 90 (1989) 3843–3854.
46 L. Song and J.M. Schurr, Biopolymers 30 (1990) 299–237.
47 B.S. Fujimoto and J.M. Schurr, Nature 344 (1990) 175–178.
48 W.H. Taylor and P.J. Hagerman, J. Mol. Biol. 212 (1990) 363–376.
49 Z. Kam, N. Borochov and H. Eisenberg, Biopolymers 20 (1981) 2671–2690.
50 R.E. Harrington, J. Am. Chem. Soc. 92 (1970) 6957–6964.
51 M.E. Hogan and O. Jardetzky, Proc. Natl. Acad. Sci. USA 76 (1980) 6341–6345.
52 P.-G. Wu, Ph.D. Thesis, University of Washington, Seattle, WA, 1988.
53 L. Song, B.S. Fujimoto, P.-G. Wu and J.M. Schurr, J. Mol. Biol. 214 (1990) 307–326.
54 P.G. Wu, L. Song, B.S. Fujimoto, J.B. Clendenning and J.M. Schurr, Allosteric transitions in secondary structure induced by superhelical stress, in: Laser scattering spectroscopy of biological objects, ed. B. Nemet (Proc. 2nd Int. Conf., Janus Pannonius University, Pécs, Hungary, 1989) pp. 1–19.
55 W.B. Upholt, H.B. Gray, Jr. and J. Vinograd, J. Mol. Biol. 62 (1971) 21–38.
56 J.C. Wang, J. Mol. Biol. 87 (1974) 794–816.
57 L. Song, Ph.D. Thesis, University of Washington, Seattle, WA, 1989.

58 R.L. Jones, A.C. Lanier, R.A. Keel and W.D. Wilson, Nucleic Acids Res. 8 (1980) 1613–1624.
59 C.E. Swenberg, S.E. Carberry and N.E. Geacintov, Biopolymers 29 (1990) 1735–1744.
60 J.H. Shibata, J. Wilcoxon and J.M. Schurr, Biochemistry 23 (1984) 1188–1194.
61 J.H. Shibata, Ph.D. Thesis, University of Washington, Seattle, WA, 1983.
62 R. Negri, F. Della Seta, E. di Mauro and G. Camilloni, Topological evidence for allosteric transitions in DNA secondary structure, preprint submitted to Biophys. J.
63 J. Langowski, A.S. Benight, B.S. Fujimoto, J.M. Schurr and U. Schomburg, Biochemistry 24 (1985) 4022–4028.
64 W. Keller, Proc. Natl. Acad. Sci. USA 72 (1975) 4876–4880.